Chapter 1 **NWP (EES 753)**
(reference)

(Based on Lin 2007; Kalnay 2003; Yu Lec. Note)

Chapter 1 Introduction and Historical Review

1.0 Introduction

Basically, *numerical weather prediction* uses numerical methods to approximate a set of partially differential equations on discrete grid points in a finite area to predict the weather systems and processes in a finite area for a certain time in the future. In order to numerically integrate the partial differential equations, which govern the atmospheric motions and processes, with time, one needs to start the integration at certain time. In order to do so, the meteorological variables need to be prescribed at this initial time, which are called *initial conditions*. Mathematically, this corresponds to solve an *initial-value problem*. Due to practical limitations, such as computing power, numerical methods, etc., we are forced to make the numerical integration for predicting weather systems in a finite area. In order to do so, it is necessary to specify the meteorological variables at the boundaries, which include upper, lower, and lateral boundaries, of the domain of interest. Mathematically, this corresponds to solve a *boundary-value problem*. Thus, mathematically, numerical weather prediction is equivalent to solving an initial- and boundary- value problem. For example, to solve the following simple one-dimensional partial differential equation,

$$\frac{\partial u}{\partial t} + U\frac{\partial u}{\partial x} = F(t,x), \tag{1.1}$$

where u is the horizontal wind speed in x-direction, U the constant basic or mean wind speed, and $F(t,x)$ is a forcing function, it is necessary to specify the u, the variable to be predicted, at an initial time, say t_o. If we are interested in the motion, to be described by u, in a finite length, we need to

specify u at one end of this finite length medium, i.e. the boundary condition.

The accuracy of the numerical weather prediction thus depends on the accuracies of the initial conditions and boundary conditions. The more accurate these conditions, the more accurate the predicted weather systems and processes. The major problems we are facing in the numerical weather prediction today is the lack of sufficient and accurate initial conditions, as well as more accurate and sufficient boundary conditions and appropriate ways in implementing them at the lateral boundaries of a finite domain of interest. One example is that we do not have enough observed data over the oceans and polar regions. Some unconventional data, such as those retrieved from radar and satellite observations, have been used to help supply the data in data-void regions. Improvement of global numerical weather prediction models is also important in improving the accuracy of the regional numerical weather prediction model since the former are often used to provide the initial and boundary conditions for the latter.

The inaccuracy of numerical weather prediction may also come from the numerical approximation of the partial differential equations governing atmospheric motions on the discrete points of a model domain, and the representation of the weather phenomena and processes occurred within grid points of a numerical model, i.e. the parameterization of subgrid-scale weather phenomena and processes. The accuracy of a numerical method can be improved by adopting a higher-order approximation of the partial differential equations used in the numerical weather prediction models, as well as using a more accurate, but stable approximation methods. These require an increase of computing power as well as better understanding of numerical approximation methods. The accuracy of subgrid-scale parameterizations can be improved by a better understanding of the weather phenomena and processes as well as reducing the grid interval of a numerical weather prediction model. Another challenge of numerical weather prediction is whether the weather systems are predictable or not. If they are intrinsically unpredictable, then the improvements in more accurate initial and boundary conditions, numerical methods, and subgrid-scale parameterizations of a numerical weather prediction will have its limitations. The weather systems are considered to have limited

predictability. Thus, it leaves us some room to make improvements of the accuracy of numerical weather prediction models.

1.1 History of Numerical Modeling in Meteorology (Ross in Ray 1986 text)

1904 V. Bjerknes -- Recognition of forecasting as an initial-value problem in mathematical physics.

1920 L. F. Richardson -- Solved the system of equations numerically using desk calculators.

1928 Courant, Friedricks and Lewy -- Found that space and time increments in integration of differential equations have to meet a certain stability criterion.

1939 Rossby -- Simplified the governing equations for large scale motion.

1950 Charney, Fjotoft and von Neumann (Charney et al., 1950) -- Made the first numerical forecasts on the ENIAC based on the Rossby's equivalent barotropic model. Only winds at 500 mb were forecasted.

1950-: Rapid advances in Numerical Weather Prediction (NWP) models.

1954: Formation of the Joint Numerical Weather Forecasting Unit for developing operational versions of research model.

1958: First geostrophic barotropic model of the Northern Hemisphere was introduced as an objective forecasting tool for NWS.

1962: A 3-level baroclinic filtered-equation (geostrophic) model became operational.

1966: A 6-level, hemispheric, primitive equation (PE) model became operational.

1971: The Limited-area Fine-Mesh (LFM) model was introduced in NMC. The horizontal resolution in North America is significantly increased.
The Nested-Grid Model (NGM) also became operational later.

1980: The grid-point hemispheric PE model was replaced by a 12 level global spectral model that predicts large-scale features for periods of 5-10 days.

1980 -: Developments of ECMWF model and ETA model.

1.2 Developments of NWP models at NCEP (Kalnay 2002)

Fig. 1.1a (Kalnay 2002) shows the longest available record of the skill of numerical weather prediction. The "S1" score (Teweles and Wobus, 1954) measures the relative error in the horizontal gradient of the height of the constant pressure surface of 500 hPa (in the middle of the atmosphere, since the surface pressure is about 1000 hPa) for 36-hour forecasts over North America. Empirical experience at NMC indicated that a value of this score of 70% or more corresponds to a useless forecast, and a score of 20% or less corresponds to an essentially perfect forecast. This was found from the fact that 20% was the average S1 score obtained when comparing analyses hand-made by several experienced forecasters fitting the same observations over the data-rich North America region.

Fig. 1.1a shows that current 36-hour 500 hPa forecasts over North America are close to what was considered essentially "perfect" 40 years ago: the computer forecasts are able to locate generally very well the position and intensity of the large-scale atmospheric waves, major centers of high and low pressure that determine the general evolution of the weather in the 36 hour forecast. The sea level pressure forecasts contain smaller-scale atmospheric structures, such as fronts, mesoscale convective systems that dominate summer precipitation, etc., and are still difficult to forecast in detail, although their prediction has also improved very significantly over the years, so their S1 score is still well above 20% (Fig.1.1b). Fig. 1.1a also shows that the 72hr forecasts of today are as accurate as the 36hr forecasts were 10-20 years ago. This doubling of skill in the forecasts (or better) is

observed for other forecast variables, such as precipitation. Similarly, 5-day forecasts, which had no useful skill 15 years ago, are now moderately skillful, and during the winter of 1997/98, ensemble forecasts for the second week average showed useful skill (defined as anomaly correlation close to 60% or higher).

The improvement in skill over the last 40 years of numerical weather prediction apparent in Fig.1.1 (Kalnay 2002) is due to four factors:

- Increased power of supercomputers, allowing much finer numerical resolution and fewer approximations in the operational atmospheric models;
- Improved representation of small-scale physical processes (clouds, precipitation, turbulent transfers of heat, moisture, momentum, and radiation) within the models;
- Use of more accurate methods of data assimilation, which result in improved initial conditions for the models; and
- Increased availability of data, especially satellite and aircraft data over the oceans and the Southern Hemisphere.

Fig. 1.1a (Sec. 1.2)

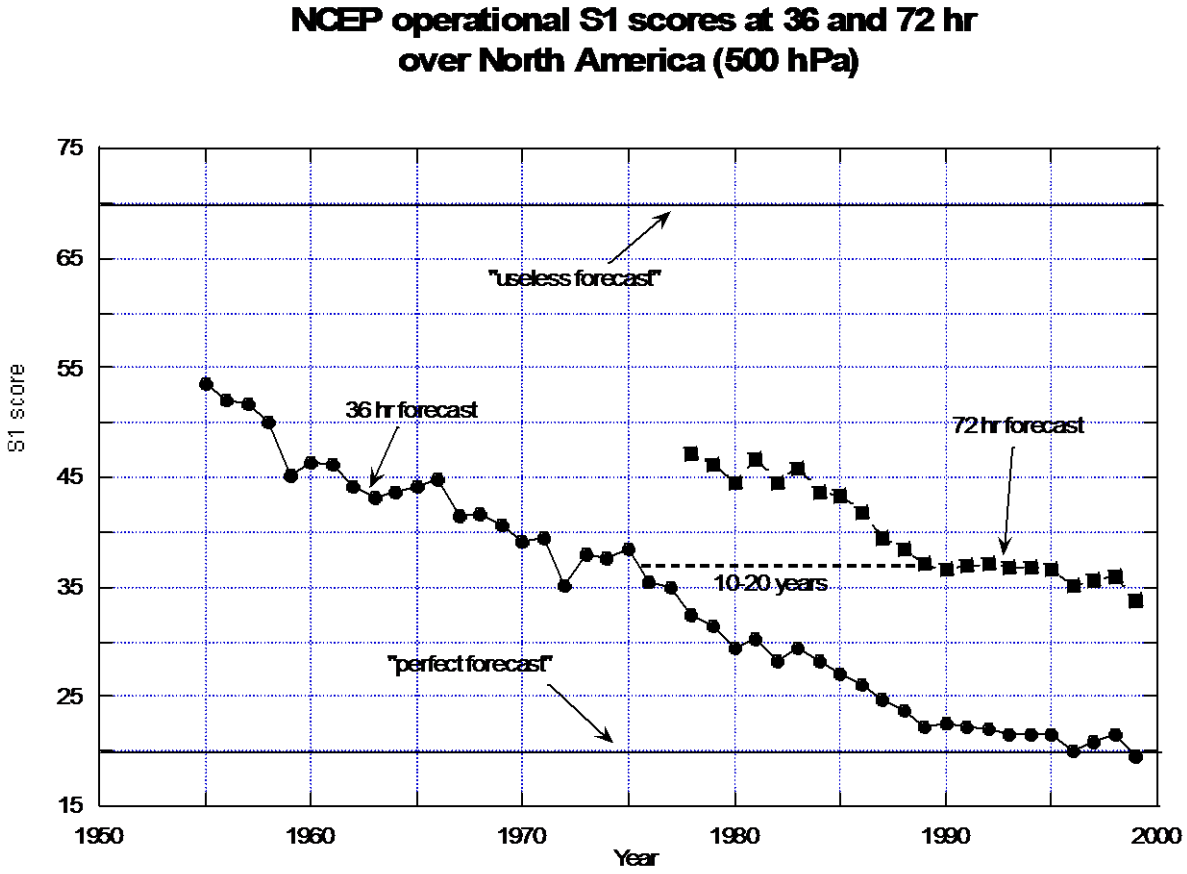

Fig. 1.1b (Sec. 1.2)

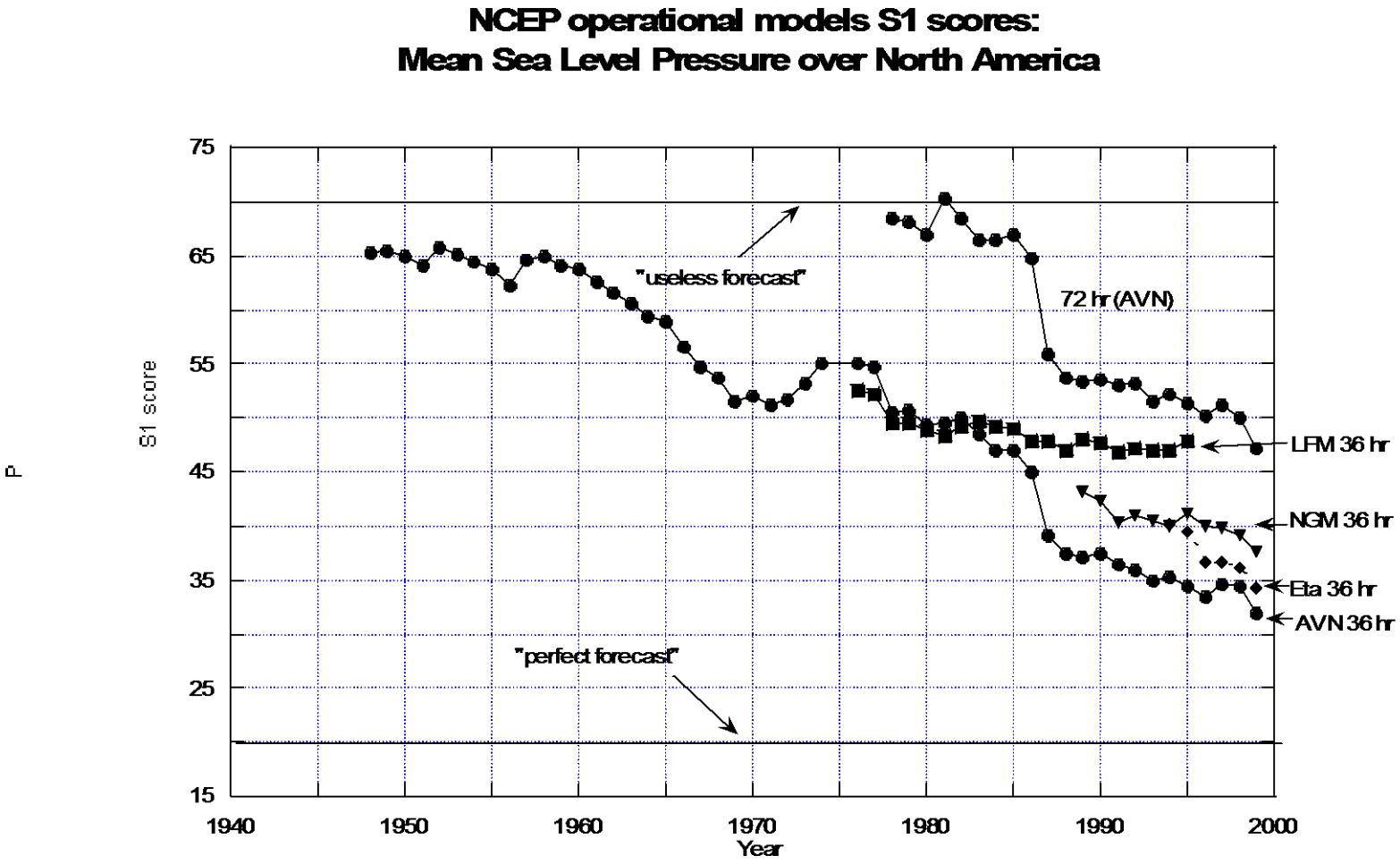

Table 1: Major operational implementations and computer acquisitions at NMC between 1955 and 1985 (adapted from Shuman, 1989)

Year	**Operational model**	**Computer**
1955	Princeton 3-level quasi-geostrophic model (Charney, 1954). Not used by the forecasters	IBM 701
1958	Barotropic model with improved numerics, objective analysis initial conditions, and octagonal domain.	IBM 704
1962	3-level quasi-geostrophic model with improved numerics	IBM 7090 (1960) IBM 7094 (1963)
1966	6-layer primitive equations model (Shuman and Hovermale, 1968)	CDC 6600
1971	Limited-area fine mesh (LFM) model (Howcroft, 1971) (first regional model at NMC)	
1974	Hough functions analysis (Flattery, 1971)	IBM 360/195
1978	7-layer primitive equation model (hemispheric)	
1978	Optimal Interpolation (Bergman1979)	Cyber 205
Aug 1980	Global spectral model, R30/12 layers (Sela, 1982)	
March 1985	Regional Analysis and Forecast System based on the Nested Grid Model (NGM, Phillips, 1979) and Optimal Interpolation (DiMego, 1988)	

Table 2: Major changes in the NMC/NCEP global model and data assimilation system since 1985 (from a compilation by P. Caplan, pers. comm., 1998)

Year	**Operational model**	**Computer acquisition**
April 1985	GFDL physics implemented on the global spectral model with silhouette orography, R40/ 18 layers	
Dec 1986	New Optimal Interpolation code with new statistics	
1987		**2nd Cyber 205**
Aug 1987	Increased resolution to T80/ 18 layers, Penman-Montieth evapotranspiration and other improved physics (Caplan and White, 1989, Pan, 1989)	
Dec 1988	Implementation of Hydrostatic Complex Quality Control (Gandin, 1988)	
1990		**Cray YMP/8cpu/ 32megawords**
Mar 1991	Increased resolution to T126 L18 and improved physics, mean orography. (Kanamitsu et al, 1991)	
June 1991	New 3D Variational Data Assimilation (Parrish and Derber, 1992, Derber et al, 1991)	
Nov 1991	Addition of increments, horizontal and vertical OI checks to the CQC (Collins and Gandin, 1990)	
7 Dec 1992	First ensemble system: one pair of bred forecasts at 00Z to 10 days, extension of AVN to 10 days (Toth and Kalnay, 1993, Tracton and Kalnay, 1993)	
Aug 1993	Simplified Arakawa-Schubert cumulus convection (Pan and Wu, 1995). Resolution T126/ 28 layers	
Jan 1994		**Cray C90/16cpu/ 128megawords**
March 1994	Second ensemble system: 5 pairs of bred forecasts at 00Z, 2 pairs at 12Z, extension of AVN, a total of 17 global forecasts every day to 16 days	
10 Jan 1995	New soil hydrology (Pan and Mahrt, 1987), radiation, clouds, improved data assimilation. Reanalysis model	
25 Oct 1995	Direct assimilation of TOVS cloud-cleared radiances (Derber and Wu, 1997). New PBL based on nonlocal diffusion (Hong and Pan, 1996). Improved CQC	**Cray C90/16cpu/ 256megawords**
5 Nov 1997	New observational error statistics. Changes to assimilation of TOVS radiances and addition of other data sources	
13 Jan1998	Assimilation of non cloud-cleared radiances (Derber et al, pers.comm.). Improved physics.	
June 1998	Resolution increased to T170/ 40 layers (to 3.5 days). Improved physics. 3D ozone data assimilation and forecast. Nonlinear increments in 3D VAR. Resolution reduced to T62/28levels on Oct. 1998 and upgraded back in Jan.2000	**IBM SV2 256 processors**

June 2000	Ensemble resolution increased to T126 for the first 60hrs	

Table 3: Major changes in the NMC/NCEP regional modeling and data assimilation since 1985 (from compilations by Fedor Mesinger and Geoffrey DiMego, pers. comm., 1998)

Year	Operational model	Computer
March 1985	Regional Analysis and Forecast System (RAFS) based on the triply Nested Grid Model (NGM, Phillips, 1979) and Optimal Interpolation (OI, DiMego, 1988). Resolution: 80 km / 16 layers.	Cyber 205
August 1991	RAFS upgraded for the last time: NGM run with only two grids with inner grid domain doubled in size. Implemented Regional Data Assimilation System (RDAS) with 3-hourly updates using an improved OI analysis using all off-time data including Profiler and ACARS wind reports (DiMego et al., 1992) and complex quality control procedures (Gandin et al., 1993).	Cray YMP 8 processors 32 megawords
June 1993	First operational implementation of the Eta Model in the 00Z & 12Z early run for North America at 80 km and 38 layer resolution (Mesinger et al., 1988, Janjic, 1994, Black et al., 1994)	
September 1994	The Rapid Update Cycle (RUC, Benjamin et al., 1994) was implemented for CONUS domain with 3-hourly OI updates at 60 km resolution on 25 hybrid (sigma-theta) vertical levels.	Cray C-90 16 processors 128 megawords
September 1994	Early Eta analysis upgrades (Rogers et al., 1995)	
August 1995	A mesoscale version of the Eta Model (Black,1994) was implemented at 03Z and 15Z for an extended CONUS domain, with 29 km and 50 layer resolution and with NMC's first predictive cloud scheme (Zhao and Black, 1994) and new coupled land-surface-atmosphere package (2 layer soil).	Cray C-90 16 processors 256 megawords
October 1995	Major upgrade of early Eta runs: 48 km resolution, cloud scheme and Eta Data Assimilation System (EDAS) using 3-hourly OI updates (Rogers et al., 1996)	
January 1996	New coupled land-surface-atmosphere scheme put into early Eta runs (Chen et al., 1997, Mesinger 1997)	
July-August 1996	Nested capability demonstrated with twice-daily support runs for Atlanta Olympic Games with 10 km 60 layer version of Meso Eta.	
February 1997	Upgrade package implemented in the early and Meso Eta runs.	
February 1998	Early Eta runs upgraded to 32 km and 45 levels with 4 soil layers. OI analysis replaced by 3-Dimensional Variational (3D VAR) with new data sources. EDAS now partially cycled (soil moisture, soil temperature, cloud water/ice & turbulent kinetic energy).	
April 1998	RUC (3-hourly) replaced by hourly RUC II system with extended CONUS domain, 40 km & 40 level resolution, additional data sources and extensive physics upgrades.	

June 1998	Meso runs connected to early runs as single 4 / day system for North American domain at 32 km and 45 level resolution, 15z run moved to 18z, added new snow analysis. All runs connected with EDAS, which is fully cycled for all variables.	**IBM SV2 256 processors**

1.3 Developments in mesoscale models and cloud models.

(a) Mesoscale research models (some examples)

PSU/NCAR MM4 (Anthes et al., 1982; Kuo and Anthes, 1984);
MASS (Kaplan et al., 1982);
GFDL models (Orlanski et al., 1983; Orlanski and Polinsky, 1984);
Drexel LAMPS (Kalb, 1984; Chang et al., 1984);
Hurricane Research Division Model;
CSU Mesoscale Model (Pielke et al.);
Australian CSIRO model (Physick et al.);
French MC2 model (Blondin et al.);
NMC models;
Naval Environmental Research Facility model;
NOAA/ERL model;
UK Meteorological Office Mesoscale Model;
and models developed in universities.

(b) Cloud Model

Clark Model, Wilhelmson and Klemp model, Schlesinger model, Orville model, Cotton model, Meso-NH, TASS, rims, NH-MASS, etc.

(c) Merged Mesoscale-Cloud Model

CSU-RAMS model, PSU/NCAR MM5 model, ARPS model, COAMPS, Nonhydrostatic MASS, Meso-NH (France), etc.

1.4 Introduction to Mesoscale Meteorology

Mesoscale meteorology or *mesometeorology* is defined in the Glossary of Meteorology (Huschke 1959) as "that portion of meteorology concerned with the study of atmospheric phenomena on a scale larger than that of *micrometeorology*, but smaller than the *cyclonic scale*." Traditionally, the cyclonic scale is also called the *synoptic scale*, *macroscale*, or *large scale*. Based on this definition, the Glossary of Meteorology further elucidates that mesometeorology is concerned with the detection and analysis of the state of the atmosphere, as it exists between meteorological stations, or at least well beyond the range of normal observation from a single location.

The types of major weather phenomena that are small enough to remain undetected within a standard observational network are sometimes called "mesometeorological", such as thunderstorms, cumulus clouds and immature tropical cyclones. The study of atmospheric phenomena based on the use of meteorological data obtained simultaneously over the standard observational network is then called *synoptic meteorology*. Synoptic scale phenomena include long waves, and cyclones. Traditionally, these scales have been loosely used or defined. For example, the tornado is classified as a mesometeorological phenomenon by the Glossary of Meteorology, while it is generally classified as a microscale meteorological phenomenon elsewhere (e.g. Ligda 1951; Orlanski 1975). Other examples are fronts and hurricanes, which have been classified as macroscale phenomena by some scientists (e.g. Stull 1988), but are classified as mesoscale phenomena by others (e.g. Orlanski 1975; Thunis and Bornstein 1996).

Due to the lack of observational data at the mesoscale, mesoscale meteorology has advanced less rapidly compared to synoptic meteorology. For example, some isolated, unusual values of pressure, winds, etc., shown on synoptic charts are suspected to be observational errors. Even though this may be true in some cases, others may represent true signatures of subsynoptic disturbances having spatial and temporal scales too small to be properly analyzed and represented on standard synoptic charts. However, due to the advancement of observational techniques and an overall increase

in the number of mesoscale observational networks over the past two decades, more and more mesoscale phenomena, as well as their interactions with synoptic scale and microscale flows and weather systems, have been revealed and better understood. In order to improve mesoscale weather forecasting, it is essential to improve our understanding of the dynamics of mesoscale atmospheric phenomena through fundamental theoretical and modeling studies. Since the mesoscale spans horizontal scales from 2 to 2000 km (e.g. Orlanski, 1975), there is no single theory, such as quasi-geostrophic theory for the large scale, which provides a unique tool for studying the dynamical structure of the variety of mesoscale motions observed in the Earth's atmosphere. Since the dominant dynamical processes vary dramatically from system to system, depending on the type of mesoscale circulation system involved.

1.5 Definitions of Atmospheric Scales

Due to different force balances, atmospheric motions behave differently for fluid systems with different temporal and spatial scales. In order to better understand the complex dynamical and physical processes associated with mesoscale phenomena, different approximations have been adopted to help resolve the problems. Therefore, a proper scaling will facilitate the choice of appropriate approximations of the governing equations.

Scaling of atmospheric motions is normally based on observational and theoretical approaches. In the observational approach, atmospheric processes are categorized through direct empirical observations and the utilities used. Since observational data are recorded in discrete time intervals and the record of these data in the form of a standard surface or upper air weather map reveals a discrete set of phenomena, the phenomena are then also categorized into discrete scales. For example, sea breezes occur on time scales of ~1 day and spatial scales of 10 to 100 km, while cumulus convection occurs on a time scale of ~30 minutes and encompasses a spatial scale of several kilometers (km).

Figure 1.1 shows the atmospheric kinetic energy spectrum for various time scales (Vinchenko, 1970). There are strong peaks at frequencies ranging from a few days (the synoptic scale) to a few weeks (the planetary scale). There are also peaks at 1 year and 1 day and a smaller peak at a few minutes (although this latter peak may be an artifact of the analysis). This energy spectrum therefore suggests a natural division of atmospheric phenomena into three distinct (but not wholly separable) scales: *macroscale, mesoscale, and microscale*. From the kinetic energy spectrum (Fig. 1.1), the mesoscale therefore appears as the scale on which energy is allowed to transfer from the large (i.e. synoptic) scale to the small (i.e. micro) scale and vice versa.

Based on radar storm observations, Ligda (1951) categorized atmospheric motions into the following scales: (a) microscale: $L < 20$ km, (b) mesoscale: 20 km $< L <$ 1000 km, and (c) synoptic scale: $L >$ 1000 km, where L represents the horizontal scale of the atmospheric motions. Orlanski (1975) proposed a more detailed classification scheme and suggested that atmospheric motions be categorized into eight (8) separate scales, namely, macro-α ($L >$ 10,000 km), macro-β (10,000 km $> L >$ 2000 km), meso-α (2000 km $> L >$ 200 km), meso-β (200 km $> L >$ 20 km), meso-γ (20 km $> L >$ 2 km), micro-α (2 km $> L >$ 200 m), micro-β (200 m $> L >$ 20 m), and micro-γ ($L <$ 20 m) scales (see Table 1.1). In addition, Fujita (1981) has proposed 5 scales of atmospheric phenomena, namely masocale, mesoscale, misoscale, mososcale, and musoscale.

Atmospheric motions may also be categorized using a theoretical approach. For example, for airflow over a mountain or a lake, the scales of the mechanically or thermally induced waves correspond to the scales of the imposed forcing. For such problems, adoption of the *Eulerian* (fixed in space) *time scale* is reasonable. For two steady cumulus clouds being advected by a steady basic zonal (i.e. westerly) wind, the time scale for a stationary observer located on the ground is approximately *L/U=1000 s*. However, the above time scale has little to do with the physics of clouds. It is more meaningful physically to use the *Lagrangian time scale*, which gives the scale following the fluid motion. In the above example, the

Lagrangian time scale is the time for an air parcel to rise to its maximum vertical extent. Another example is the Lagrangian time scale for a cyclone, which is defined as the circumference an air parcel travels ($2\pi R$) divided by the tangential wind speed. The Lagrangian time scales and Rossby numbers for typical atmospheric systems are summarized below.

	T	Lagrangian R_o $(\sim \omega/f = 2\pi/fT)$
Tropical cyclone	$2\pi R/V_T$	V_T/fR
Inertia-gravity waves	$2\pi/N$ to $2\pi/f$	N/f to 1
Sea/land breezes	$2\pi/f$	1
Thunderstorms and cumulus clouds	$2\pi/N_w$	N_w/f
Kelvin-Helmholtz waves	$2\pi/N$	N/f
PBL turbulence	$2\pi h/U^*$	U^*/fh
Tornadoes	$2\pi R/V_T$	V_T/fR

where

R = radius of maximum wind wind scale,
V_T = maximum tangential wind scale,
f = Coriolis parameter,
N = buoyancy (Brunt-Vaisala) frequency,
N_w = moist buoyancy frequency,
U^* = scale for friction velocity,
h = scale for the depth of planetary boundary layer.

Based on the above theoretical considerations, Emanuel and Raymond (1984) define the following different scales: (a) synoptic scale - for motions which are quasi-geostrophic and hydrostatic, (b) mesoscale – for motions which are *non*quasi-geostrophic and hydrostatic, and (c) microscale – for motions which are non-geostrophic, nonhydrostatic, and turbulent. Therefore, based on this interpretation, the mesoscale may be defined as that scale which includes atmospheric circulations, which are large enough in horizontal scale to be considered hydrostatic, but too small to be described quasi-geostrophically.

Arya (1988) defines micrometeorological phenomena as being limited to those that "originate in and are dominated by" the planetary boundary layer, excluding phenomena whose "dynamics are largely governed by mesoscale and macroscale weather systems." Taking a similar approach, Pielke (1984) defines mesoscale phenomena as having a horizontal length scale large enough to be considered hydrostatic but small enough so that the Coriolis force is small relative to the nonlinear advective and horizontal pressure gradient forces. In fact, Pielke's definition of mesoscale phenomena coincides with the meso-β scale as defined by Orlanski (1975). Orlanski's meso-α and macro scales are further divided into regional and synoptic scales in Pielke's classification. Stull (1988) defines the mesoscale in much the same way as does Orlanski, but with the microscale defined as 2 m < L < 3 km and an additional micro-δ scale for L < 2 m.

Recently, Thunis and Bornstein (1996) take a more rigorous approach based on hydrostatic, convective, advective, compressible, and Boussinesq approximations of the governing equations, including temporal, horizontal and vertical spatial scales, to standardize existing nomenclature with regard to mesoscale phenomena. Their work integrates existing concepts of atmospheric spatial scales, flow assumptions, governing equations, and resulting motions into a hierachy useful in the categorization of mesoscale models. Horizontal and vertical scales of flow subclasses under stable and unstable stability conditions for deep and shallow convection are shown in Figures 1.2 and 1.3, respectively. Thunis and Bornstein's definition of atmospheric scales are the same as those proposed by Orlanski except that Orlanski's micro-γ scale is divided into micro-γ (2 m < L < 20 m) and micro-δ (L < 2 m) scales. Table 1.1 shows the horizontal and temporal scales for typical atmospheric phenomena as proposed by Thunis and Bornstein (1996), Orlanski (1975), Pielke (1984), and Stull (1988). In this book, we will adopt Orlanski's scaling except where otherwise specified.

1.6 Energy Generation and Scale Interaction

Although many mesoscale circulations and weather systems are forced by large scale or microscale flow, some circulations are locally forced at the mesoscale itself. Energy generation mechanisms for mesoscale circulations and weather systems may be classified into the following categories (Anthes 1986; Holton 1992): (a) thermal or orographic surface inhomogeneities, (b) internal adjustment of larger-scale flow systems, (c) mesoscale instabilities, (d) energy transfer from either the macroscale or microscale to the mesoscale, and (e) interaction of cloud physical and dynamical processes.

Examples of the first type of mesoscale weather systems are the land/sea breezes, mountain-valley winds, mountain waves, heat island circulations, coastal fronts, dry lines, and moist convection. These mesoscale weather systems are more predictable than other types of systems that occur on the mesoscale. Examples of the second type of weather systems are fronts, cyclones, and jet streaks. These weather systems are less predictable since they are generated by transient forcing associated with larger-scale flows. Although instabilities associated with the mean velocity or thermal structure of the atmosphere are a rich energy source of atmospheric disturbances, most atmospheric instabilities have their maximum growth rates either on the large scale through baroclinic, barotropic, and inertial instabilities or on the microscale through *Kelvin-Helmholtz* and *convective instabilities*, symmetric instability appears to be an intrinsically mesoscale instability.

Energy transfer from small scales to the mesoscale also serves as a primary energy source for mesoscale convective systems. For example, mesoscale convective systems may start as individual convective cells, which grow and combine to form thunderstorms and convective systems, such as squall lines, mesocyclones, mesoscale convective complexes, and hurricanes. On the other hand, energy transfer from the macroscale to the mesoscale also serves as an energy source to induce mesoscale circulations or weather systems. For example, temperature and vorticity advection associated with large-scale flow systems may help develop mesoscale frontal systems. Another possible energy source for producing mesoscale circulations or weather systems is the interaction of cloud physical and

dynamical processes, and mesoscale convective systems may be generated by this interaction process through scale expansion.

Scale interaction generally refers to the interactions between the temporally and zonally averaged zonal flow and a fairly limited set of waves that are quantized by the circumference of the earth, while it refers to multiple interactions among a continuous spectrum of eddies of all sizes in turbulence theory (Emanuel 1986). However, scale interaction should not be viewed as a limited set of interactions among discrete scales, because on average, the mesoscale is much more like a continuous spectrum of scales. Scale interaction depends on the degree of relative strength of fluid motions involved. For example, for a very weak disturbance embedded in a slowly varying mean flow, the interaction is mainly exerted from the mean flow to the weak disturbance. If this disturbance becomes stronger, then it may exert an increasing influence on the mean flow, and other scales of motion may develop. In this case, scale interactions become more and more numerous, and the general degree of disorder in the flow becomes greater. At the extreme, when the disturbance becomes highly nonlinear, such as in fully developed turbulent flow, then the interactions become mutual and chaotic, and an explicit mathematical or analytic description of the interaction becomes problematic.

Examples of scale-interactive processes which occur at mesoscale are (Koch 1997): (i) synoptic forcing of mesoscale weather phenomena, (ii) generation of internal mesoscale instabilities, (iii) interactions of cloud and precipitation processes with mesoscale dynamics, (iv) influence of orography, boundary layer, and surface properties on mesoscale weather system development and evolution, (v) feedback contributions of mesoscale systems to larger-scale processes, (vi) energy budgets associated with mesoscale systems, and (vii) mechanisms and processes associated with stratosphere-troposphere exchange. Figure 1.4 shows the mutual interactions between a jet streak, inertia-gravity waves, and strong mesoscale convection, which can occur on the mesoscale (Koch 1997).

Figure 1.5 shows the energy transfer process in the response of the free atmosphere to a cumulus cloud, which radiates gravity waves and lead to a

lens of less stratified air whose width is the Rossby radius of deformation (*NH/f*). The Rossby radius of deformation is the horizontal scale at which rotational effects becomes as important as buoyancy effects (Gill, 1982). The Rossby radius of deformation can be understood as the significant horizontal scale (e-folding value) fluid parcels experience when the fluid undergoes geostrophic adjustment to an initial condition such as

$$\eta = -\eta_o \,\mathrm{sgn}(x), \qquad (1.3.1)$$

where *sgn* is defined as *sgn(x)*=1 for $x \geq 0$ and -1 for $x<0$. The process from state (a) to (b) in Fig. 1.5 represents a scale interactive process in which the system tends to reach geostrophic equilibrium with a horizontal scale of *NH/f*. The above example of cumulus convection implies as least two (2) distinct scales are involved: (i) the cumulus scale ~ *H*, and (ii) the large (or synoptic) scale ~ *NH/f* (*Rossby radius of deformation*).

1.7 Predictability

In numerical weather prediction or atmospheric modeling in general, the question of predictability concerns the degree to which a hydrodynamical model of the atmosphere will yield diverging solutions when integrated in time using slightly different initial conditions (e.g. Ehrendorfer and Errico 1995). The weather phenomenon of interest is considered to have *limited predictability* if the solutions diverge, since there is an uncertainty associated with initial conditions determined from real observations. The question of predictability of mesoscale atmospheric phenomena was first investigated by Lorentz (1969) by using a simple model for the interaction of barotropic vorticity perturbations encompassing a number of diverse horizontal scales. Those results suggested that the mesoscale may be less predictable, (i.e. yielding perturbed solutions that diverge faster), than the synoptic and planetary scales, essentially because the eddy timescale decreases with horizontal scale. The predictability for synoptic scales is mainly limited by the nonlinear interaction between different components of the wave spectrum. These interactions depend on the initial distribution of energy in the different wavenumbers and on the number of waves the model

can resolve. Errors and uncertainties in the resolvable scale waves and errors introduced by neglecting unresolvable scales grow with time and spread throughout the spectrum, eventually contaminating all wavelengths and destroying the forecast (Anthes 1986). The predictability for mesoscale motions is mainly limited by the rapid transfer of energy between the large scale and the microscale. In addition, the predictability for small scales is mainly limited by three-dimensional turbulence. Inevitable errors or uncertainties in initial conditions in the small scale of motion will propagate toward larger scales and will reach the mesoscale sooner than the synoptic scale, therefore rendering the mesoscale less predictable.

The response of a fluid system to a steady forcing tends to fall into one of the following four categories (Emanuel and Raymond 1984): (1) steady for a stable system - perfectly predictable, (2) periodic for a weakly unstable system - perfectly predictable, (3) aperiodic with a "lumpy" spectrum for a moderately unstable system - less predictable, (4) aperiodic with a monotonic spectrum for a fully turbulent system - rather unpredictable. The atmospheric system falls into category (3). Monotonicity of the (kinetic) energy spectrum (Fig. 1.1) through the mesoscale implies that the energy may be generated intermittently at the mesoscale, but mainly transferred from larger (macroscale) and smaller (microscale) scales. This tends to limit the predictability at the mesoscale. However, according to Anthes et al. (1985), the mesoscale is inherently more predictable than the larger scales, presumably because mesoscale phenomena are strongly constrained by topography and other surface features. Such constraints may only work when other dynamical processes are weak.

Beside the natural constraints imposed by forcing and physical processes, predictability of mesoscale phenomena is also affected by the initial conditions set up in a mesoscale numerical prediction model. If a mesoscale phenomenon does not exist at the beginning of the numerical prediction, then the predictability is less influenced by the accuracy of the initial conditions used in a mesoscale numerical weather prediction model. Under this situation, the mesoscale circulations are normally forced by surface inhomogeneities (thermal or orographic), internal adjustment of

larger-scale flow systems, mesoscale instabilities, energy transfer from either the macroscale or the microscale, or the interaction of cloud physical and dynamical processes, as discussed earlier.

Since the mesoscale circulation is induced by the larger scale motion, the time scale for predictability of these types of mesoscale systems could exceed the actual time scale of the mesoscale systems themselves. On the other hand, if a mesoscale phenomenon exists at the beginning of the numerical prediction, then it is necessary to include the observed and analyzed motion and thermodynamic variables in the initial conditions in order to make an accurate numerical prediction. In this case, the roles played by the numerical model and observations may be depicted by Fig. 1.6. The theoretical limit of prediction decreases with time from 100% at the beginning of prediction. The accuracy of the numerical prediction relies more on observations in the beginning and less on the model because it takes time for the model to spin up. Thus, observations are more important than the numerical model in the beginning of the numerical prediction. Contributions of the model become more and more important as time proceeds.

References

Anthes, R. A., 1986: The general question of predictability. In *Mesoscale Meteorology and Forecasting*, Ed. P. S. Ray, Amer. Meteor. Soc., 636-656.

Arya, P., 1988: *Introduction to Micrometeorology*. Academic Press, 307 pp.

Ehrendorfer, M., and R. M. Errico, 1995: Mesoscale predictability and the spectrum of optimal perturbations. *J. Atmos. Sci.*, 52, 3475-3500.

Emanuel, K., 1986: Overview and definition of mesoscale meteorology. In *Mesoscale Meteorology and Forecasting* (P. S. Ray, Ed.), 1-16.

Emanuel, K., and D. J. Raymond, 1984: *Dynamics of Mesoscale Weather Systems*. Ed. J. B. Klemp, NCAR, 1984.

Fujita, T. T., 1981: Tornadoes and downbursts in the context of generalized planetary scales. *J. Atmos. Sci.*, 38, 1512-1534.

Fujita, T. T., 1986: Mesoscale classifications: Their history and their application to forecasting. In *Mesoscale Meteorology and Forecasting* (P. S. Ray, Ed.), 18-35.

Gill, A. E., 1982: *Atmosphere-ocean dynamics*. Academic Press. 662 pp.

Holton, J. R.: *Introduction to Dynamic Meteorology*. Academic Press, Inc. 511pp.

Huschke, R. E., 1959 (Ed.): *Glossary of Meteorology*, 3rd Edition, Amer. Meteor. Soc., 638pp.

Koch, S. E., 1997: Atmospheric Convection. Lecture notes, North Carolina State University.

Ligda, M.G.H., 1951: Radar storm observations. Compendium of Meteorology, AMS, Boston, Mass, 1265-1282.

Lorentz, E. N., 1969: The predictability of a flow which possesses many scales of motion. *Tellus*, 21, 289-307.

Orlanski, I., 1975: A rational subdivision of scales for atmospheric processes. *Bull. Amer. Meteor. Soc*., **56**, 527-530.

Ray, P. S., 1984: *Mesoscale Meteorology and Forecasting*. Amer. Meteor. Soc., 793pp.

Stull, R., 1988: *An Introduction to Boundary Layer Meteorology*. Kluwer Academic, 666pp.

Thunis, P. and R. Bornstein, 1996: Hierachy of mesoscale flow assumptions and equations. *J. Atmos. Sci*., 53, 380-397.

UCAR, 1983: The National STORM Program: Scientific and Technical Bases and Major Objectives. University Corporation for Atmospheric Research. 8-30pp.

Vinnichenko, N. K., 1970: The kinetic energy spectrum in the free atmosphere - one second to five years. *Tellus*, 22, 158-166.

Table Captions

Table 1: Atmospheric scale definitions, where L_H is horizontal scale length. (adapted from Thunis and Bornstein 1996).

TABLE 1. Atmospheric scale definitions, where L_H is horizontal scale length.

L_H	Lifetime	Stull (1988)	Pielke (1984)	Orlanski (1975)	Present	Atmospheric phenomena
10 000 km	1 month	Macro	Synoptic Regional	Macro-α	Macro-α	General circulation, long waves
2000 km	1 week			Macro-β	Macro-β	Synoptic cyclones
200 km	1 day			Meso-α	Macro-γ	Fronts, hurricanes
20 km	1 h	Meso	Meso	Meso-β	Meso-β	Low-level jets, thunderstorm groups, mountain winds and waves, sea breeze, urban circulations
2 km				Meso-γ	Meso-γ	Thunderstorm, clear-air turbulence
200 m	30 min	Micro	Micro	Micro-α	Meso-δ	Cumulus, tornadoes, katabatic jumps
20 m	1 min			Micro-β	Micro-β	Plumes, wakes, waterspouts, dust devils
2 m	1 s	Micro δ		Micro-γ	Micro-γ	Turbulence, sound waves
					Micro-δ	

Figure Captions (for Sec. 1.4-1.7)

Fig. 1.1: Average kinetic energy of west-east wind component in the free atmosphere (Adapted after Vinnichenko 1970).

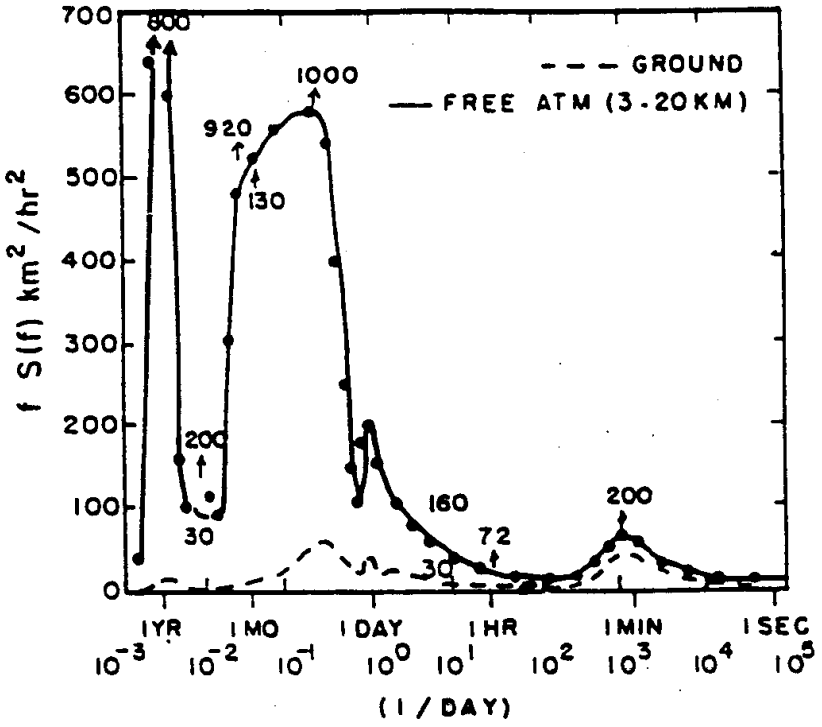

Fig. 1.2: Schematic of flow subclasses under unstable stability conditions, where hatched zones indicate that nonphysical phenomena, dotted line indicates merging of thermodynamic advection with macroscale, r represents scaled ratio of bouyancy and vertical pressure gradient forced perturbations, and dashed line represents division of thermal convection into its deep and shallow regimes. (Adapted after Thunis and Bornstein 1996)

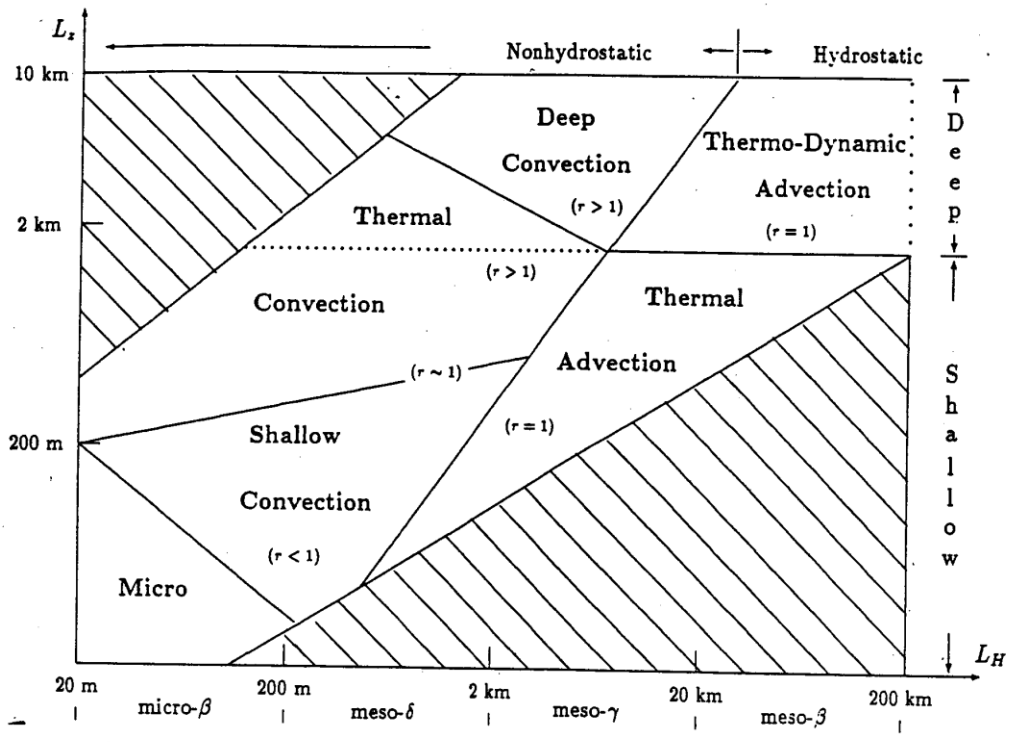

Fig. 1.3: As in Fig. 1.2 except for stable stability conditions. (Adapted after Thunis and Bornstein 1996)

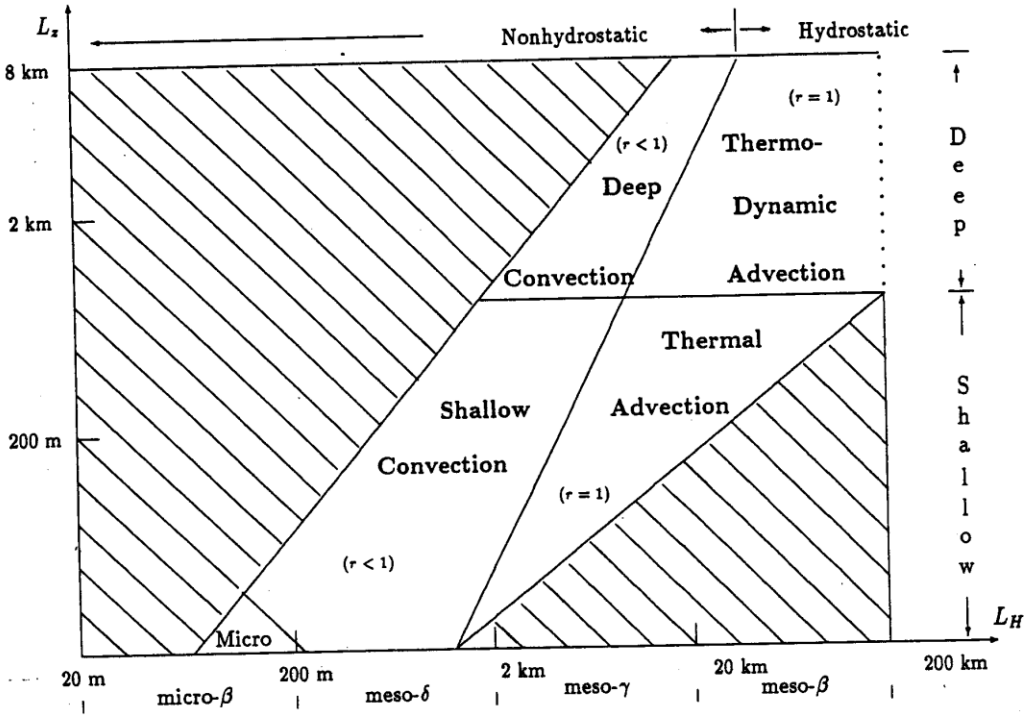

Fig. 1.4: Sketch of mutual interactions between the jet streak, inertial-gravity waves, and strong convection. (Adapted after Koch 1997)

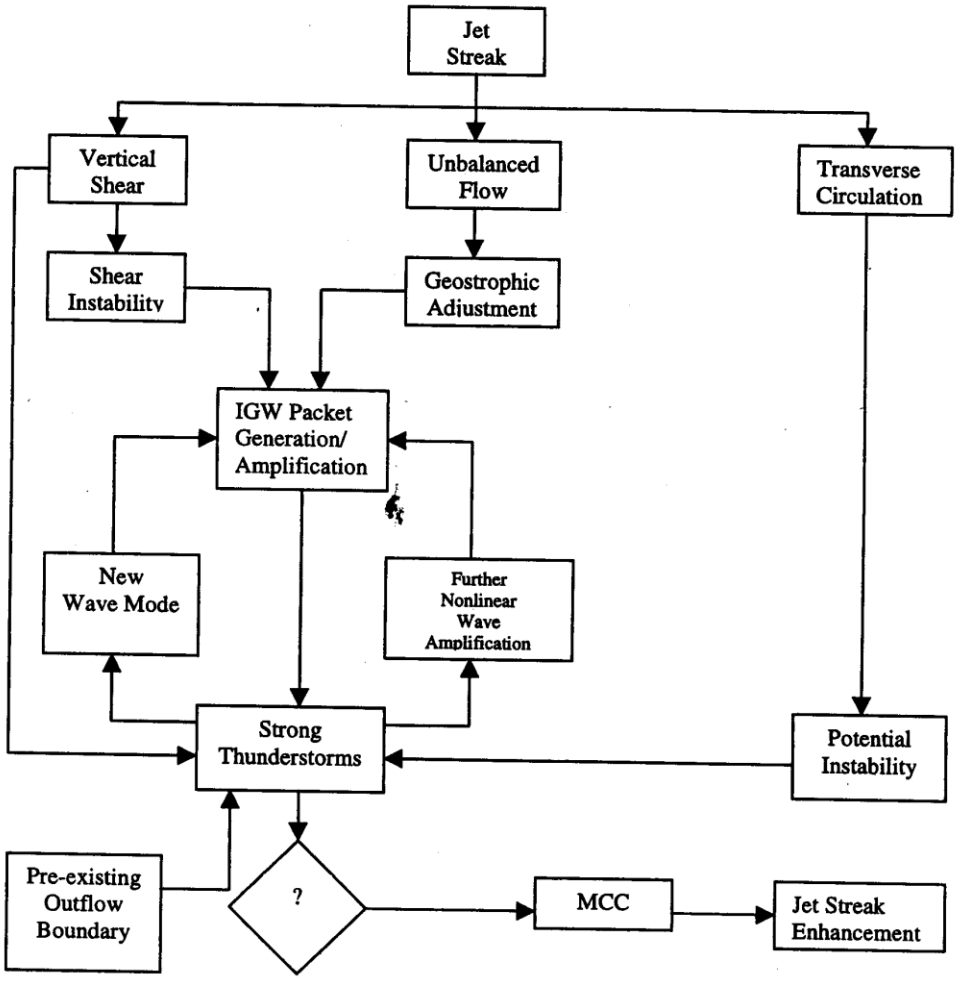

Fig. 1.5: (a) The response of the free atmosphere to a cumulus cloud is to radiate gravity waves, which lead in the end to (b) a lens of less stratified air whose width is the Rossby radius of deformation. (Adapted after Emanuel and Raymond 1984)

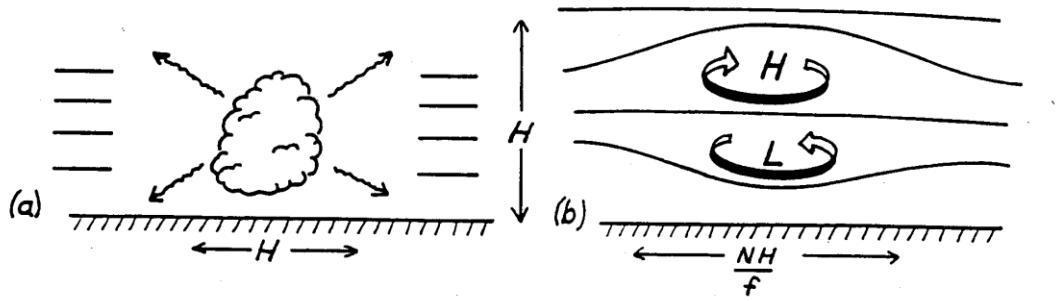

Fig. 1.6: A sketch for demonstrating the relationship between observations, numerical models, and theoretical limit of prediction. (Adapted after UCAR 1983)